Materials Science-Poland, 31(1), 2013, pp. 6-13
http://www.materialsscience.pwr.wroc.pl/
DOI: 10.2478/s13536-012-0060-x

VERSITA

Tuning photocurrent response through size control of CdSe quantum dots sensitized solar cells

A. BADAWI[1,2*], N. AL-HOSINY[1], S. ABDALLAH[1,3], H. TALAAT[2]

[1] Department of Physics, Faculty of Science, Taif University, Taif, Saudi Arabia
[2] Physics Department, Faculty of Science, Ain Shams University, Abbassia Cairo, Egypt
[3] Department of Mathematical and Physical Engineering, Faculty of Engineering (Shoubra), Benha University, Cairo, Egypt

The photovoltaic characterization of CdSe quantum dots sensitized solar cells (QDSSCs) by tuning band gap of CdSe quantum dots (QDs) through size control has been investigated. Fluorine doped tin oxide (FTO) substrates were coated with 20 nm in diameter TiO_2 nanoparticles (NPs). Pre-synthesized colloidal CdSe quantum dots of different sizes (from 4.0 to 5.4 nm) were deposited on the TiO_2-coated substrates using direct adsorption (DA) method. The FTO counter electrodes were coated with platinum, while the electrolyte containing I^-/I_3^- redox species was sandwiched between the two electrodes. The current density-voltage (J-V) characteristic curves of the assembled QDSSCs were measured for different dipping times, and AM 1.5 simulated sunlight. The maximum values of short circuit current density (J_{sc}) and conversion efficiency (η) are 1.62 mA/cm^2 and 0.29 % respectively, corresponding to CdSe QDs of size 4.52 nm (542 nm absorption edge) and of 6 h dipping time. The variation of the CdSe QDs size mainly tunes the alignment of the conduction band minimum of CdSe with respect to that of TiO_2 surface. Furthermore, the J_{sc} increases linearly with increasing intensity of the sun light, which indicates the sensitivity of the assembled cells.

Keywords: *CdSe quantum dot; tuning band gap; direct adsorption; quantum dots sensitized solar cell; photovoltaic cells*

1. Introduction

The last decade witnessed a great attention toward improvement of the performance of the third generation solar cells, especially that of quantum dots sensitized solar cells (QDSSCs) [1, 2]. In this kind of solar cells, quantum dots (QDs) are adsorbed onto large band gap metal oxides such as TiO_2 NPs [3, 4], ZnO NPs [4], and SnO_2 NPs [5] to act as sensitizers. These QDs posses many attractive properties such as the ability to tune their band gaps by controlling their sizes (therefore the absorption spectra can be tuned to match the spectral distribution of sunlight [6]) and high extinction coefficients due to quantum confinement effects [3, 7]. Additionally, they have large intrinsic dipole moment, leading to rapid charge separation [6, 8], intrinsically stronger absorbers [9], unique electronic and optical properties [10], low manufacturing cost [11], and resistance to oxygen and water [6]. Furthermore, some of these QDs produce more than one electron-hole pair due to a single absorbed photon. It is so called multiple exciton generation (MEG) [12, 13]. These factors raise the theoretical maximum efficiency above the Shockley-Queisser limit of 31 % [7]. QDSSCs have larger surface areas and provide a technically and economically credible alternative to conventional cells, silicon photovoltaic or dye-sensitized solar cells (DSSCs). The latter cells have many limitations, such as difficulties in utilizing the infrared region of the solar spectrum, and instability for long-term uses. Several works were carried out using QDs as photosensitizers such as: CdS [14, 15], CdSe [16], CdTe [17], PbSe [18]], PbS [19], InAs [20], ZnSe [21], $Cu_{2-x}S$ [22], Ag_2S [3], and Ag_2Se [23].

CdSe QDs are relatively easy synthesized and size controllable, which makes possible to tune their band gaps to harvest more light energy in the visible region of the solar spectrum. Bulk CdSe has high absorption coefficient ($\sim 10^4$ cm^{-1} [24]) in the visible light region. Furthermore, its conduction band (CB)

*E-mail: adaraghmeh@yahoo.com

(−4.3 eV *vs.* vacuum [25]), an ionization potential of −6.04 eV *vs.* vacuum [25] and direct band gap energy of 1.74 eV [10]) would behave as a good sensitizer capable of effectively injecting electrons to TiO_2 NPs (bulk TiO_2 band gap is 3.2 eV [4, 25]). These characteristics make CdSe QDs an appropriate sensitizer to check the QDSSCs concepts [26].

Essentially, two different strategies may be used to deposit QDs onto the large band gap metal oxides [27]: in situ growth of QDs by either chemical bath deposition (CBD) method, containing both cationic and anionic precursors [6, 23], or successive ionic layer adsorption and reaction deposition (SILAR) method [9]. These methods provide good surface coverage, but the control over the QD size is limited and the size distribution is broad [28]. These drawbacks can be avoided if the QDs are synthesized earlier (*ex situ*) [14], and then deposited by electrophoretic deposition (EPD) [28], linker-assisted adsorption (LA) [29], and direct adsorption (DA) [11] for different dipping times.

In this work, we prepared CdSe QDs of different sizes by chemical deposition (CD) technique to be used as a sensitizer in QDSSCs. These colloidal QDs were adsorbed onto TiO_2 NPs by DA technique for different dipping times under ambient conditions. The effect of the CdSe QDs size on the QDSSCs characteristic parameters (short circuit current density (J_{sc}), open circuit voltage (V_{oc}), fill factor (FF), and efficiency for energy conversion (η) were studied. Furthermore, the performance of the assembled CdSe QDSSCs under different percentages of sun was studied.

2. Experiment

2.1. Synthesis of CdSe quantum dots

Colloidal CdSe nanocrystals were prepared by the method of Talapin *et al.* [30]. We used hexadecylamine (HDA) as a capping agent, together with trioctylphosphine oxide (TOPO) to facilitate the preparation of highly monodisperse nanocrystals (size distribution 5 %). Five samples of different sizes, ranging from 4 to 5.4 nm, were obtained at five time intervals from the same synthesis, and labeled (a to e). All the samples were immediately cooled and rinsed with toluene.

2.2. Preparation of solar cell electrodes

Colloidal paste of TiO_2 was prepared by the method of G. Syrrokostas *et al.* [31], as follows: 3 grams of commercial TiO_2 nanopowder (20 nm) (Degussa P-25 titanium dioxide consists of 80 % anatase and 20 % rutile) were ground in a porcelain mortar and mixed with a small amount of distilled water (1 ml) containing acetyl acetone (10 % v/v) to create the paste. Acetyl acetone was used as a dispersing agent, since it prevents coagulation of TiO_2 nanoparticles and affects the porosity of the film. The paste was diluted further by slow addition of distilled water (4 ml) under continued grinding. The addition of water controlled the viscosity and the final concentration of the paste. Finally, a few drops of a detergent (Triton X-100) were added to facilitate the spreading of the paste on the substrate, since this substance has the ability to reduce surface tension, resulting in even spreading and reducing the formation of cracks. The TiO_2 paste was deposited on a transparent conducting glass substrate of SnO_2:F (FTO) with a sheet resistance of 7 Ω/sq and transmittance > 80 % in the visible region, using doctor blade technique. This was followed by annealing at 450 °C for 30 min, and the final thickness was 8 μm after the solvent evaporation. Then the TiO_2 films were directly dipped into a colloidal solution of each pre-synthesized size of CdSe QDs to form five working electrodes. The counter electrodes were prepared by coating another FTO substrate sheets with Pt.

2.3. Assembly of CdSe QDSSC

CdSe QDs sensitized TiO_2 electrode and Pt counter electrode were assembled as a sandwich type cell using clamps. Both electrodes were sealed using a hot-melt polymer sheet (solaronix, SX1170-25PF) of 25 μm thickness in order to avoid evaporation of the electrolyte. Finally, the iodide electrolyte solution was prepared by dissolving 0.127 g of 0.05 M iodine (I_2) in 10 mL of water-free ethylene glycol, then adding 0.83 g of 0.5 M potassium iodide (KI). The electrolyte was inserted in the cell with a syringe, filling the space between the two electrodes.

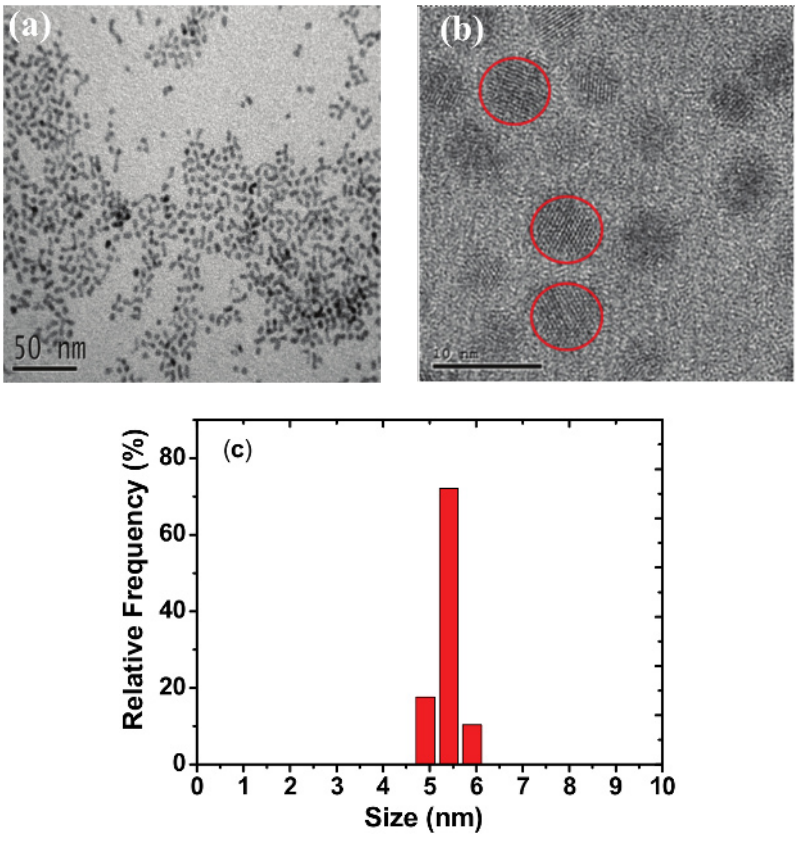

Fig. 1. Results of characterization for sample e: (a) TEM micrograph; (b) HRTEM micrograph, and (c) histogram of particle size distribution.

2.4. Measurements

The absorption spectra of the CdSe QDs (before and after adsorption on TiO_2 electrodes) were recorded using a UV-Visible spectrophotometer (JASCO V-670). In addition, the sizes of the QDs were measured with a high resolution transmission electron microscope (HRTEM). The current density-voltage (J-V) characteristics were recorded with a Keithley 2400 voltage source/ammeter using GreenMountain IV-Sat 3.1 software, when the CdSe QDSSCs were subjected to the illumination of a solar simulator (ABET technologies, Sun 2000 Solar Simulators, USA) operating at 100 mW/cm^2 (AM1.5G). The intensity of the incident solar illumination was adjusted to 1 sun condition using a Leybold certified silicon reference solar cell (Model: 57863 Solar cell 2 V/0.3 A STE 4/100). The J-V characteristic curves of all five sizes of CdSe QDSSCs (after 6 hours dipping time) were studied at various illumination intensities using attenuators and adjusted by the previous Si reference solar cell. All experiments were carried out under ambient conditions.

3. Results and discussion

3.1. Characterization of the CdSe QDs

The average particle size of all prepared CdSe QDs, ranging from 4.0 nm for the smallest sample (a) to 5.4 nm for the largest one (e) were estimated using HRTEM. Fig. 1 (a, b, and c) shows TEM micrographs, HRTEM micrograph, and a histogram of particle size distribution for sample (e).

The UV-Vis. absorption spectra of the samples in colloidal solution were obtained and given in Fig. 2. The first excitonic absorption edges are easily observed at 509, 532, 542, 566 and 583 nm for samples (a), (b), (c), (d), and (e) respectively. The

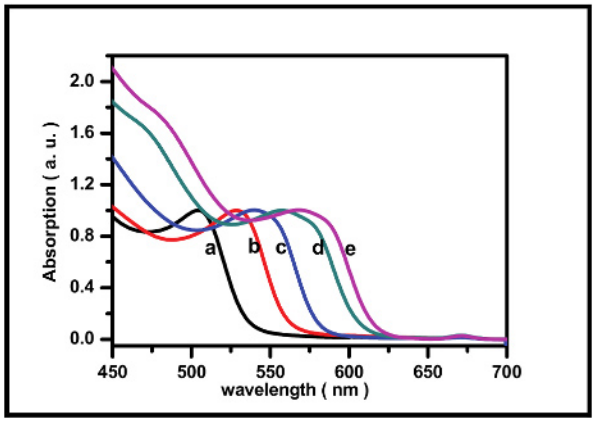

Fig. 2. UV-visible absorption spectra for CdSe QDs samples (a to e).

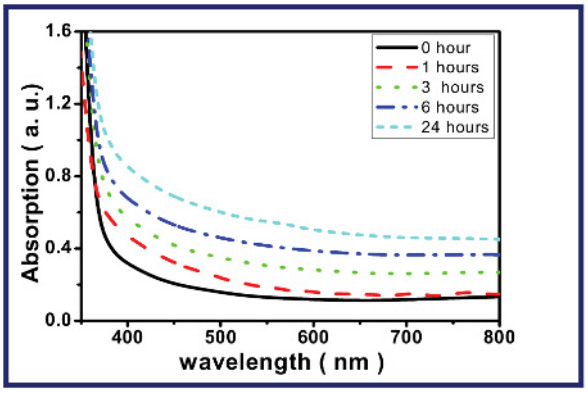

Fig. 3. UV-vis. absorption spectra of CdSe QDs (sample c) deposited on TiO_2 NPs at 0, 1, 3, 6 and 24 hour dipping time.

red shifts of the onset absorption spectra to longer wavelengths with increasing particle size are due to the varying quantum confinement effect.

The corresponding CdSe QDs radii were also calculated using the effective mass approximation (EMA) model [32]:

$$E_{g(Nano)}(R) = E_{g(bulk)} + \frac{h^2}{8R^2}\left[\frac{1}{m_e} + \frac{1}{m_h}\right] - \frac{1.8e^2}{4\pi\varepsilon\varepsilon_0 R} \quad (1)$$

where $m_e = 0.13m_0$ and $m_h = 0.45m_0$ [24] are the effective masses of electron and hole respectively, m_0 is the electron mass, $E_{g(bulk)}$ =1.74 eV [10], is the bulk crystal band gap, R is the average radius of the nanocrystal, $E_{g(Nano)}$ is the QD band gap value, h is the Plancks constant and $\varepsilon = 5.8$ [24], is the relative permittivity. The average particle sizes of CdSe QDs, estimated based on Equation (1), ranged from 4.02 nm for sample (a) to 5.20 nm for sample (e) which closely corresponded to those estimated from TEM micrographs.

3.2. Characterization of CdSe QDs sensitized TiO_2 electrodes (the working electrode)

The UV-Vis. absorption spectra of each of the working electrodes for all CdSe QDs sizes (a to e) were recorded for four dipping times (1, 3, 6, and 24 hour). As an example, Fig. 3 shows the absorption spectra of CdSe QDs (sample c) sensitized TiO_2 electrodes as a function of dipping time. It is clearly seen that the absorption increases as the adsorption time increases due to the increase in the amount of CdSe QDs loading. Furthermore, a significant shift toward the visible spectra region is also observed.

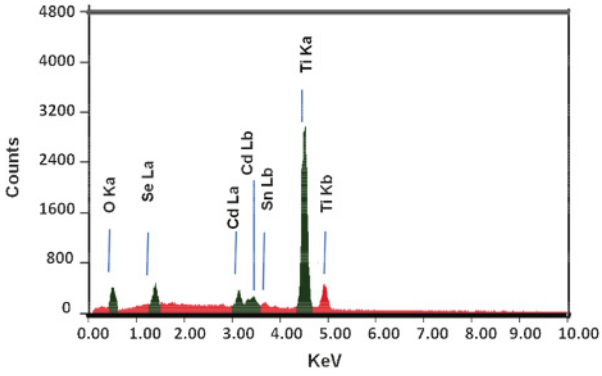

Fig. 4. EDX of CdSe QDs (sample c) adsorbed onto TiO_2 electrode.

To ensure the adsorption of CdSe QDs onto the TiO_2 electrode, EDX was performed for CdSe QDs sample (c) – TiO_2 working electrode, and the results are shown in Fig. 4, where the peaks refer to Cd and Se, in addition to Ti, Sn, and O_2.

3.3. Characterization of CdSe QDSSC

Fig. 5 shows the J-V characteristics curve of the assembled CdSe (sample c) QDSSCs for four dipping times (1 h, 3 h, 6 h, 24 h) using TiO_2 photoelectrodes and 100 mW/cm^2 from a solar simulator.

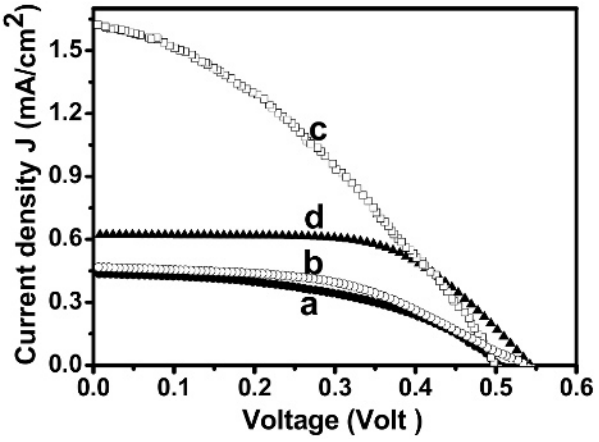

Fig. 5. J-V characteristics curves of CdSe (sample c) QDSSCs for (a) 1 h,(b) 3 h, (c) 6 h, and (d) 24 h dipping time.

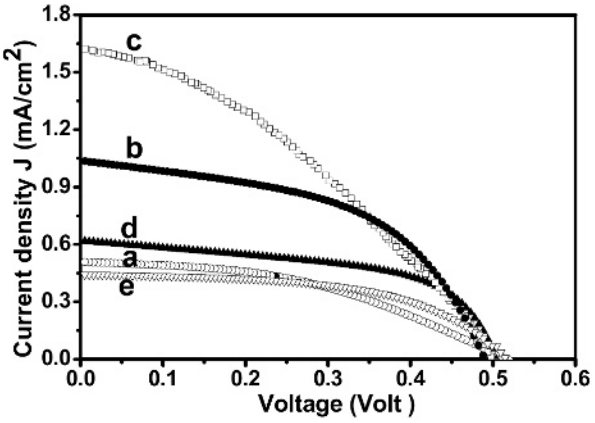

Fig. 6. J-V characteristic curve of QDSSCs of CdSe QDs with the size: (a) 4.02, (b) 4.32, (c) 4.54, (d) 4.84, and (e) 5.20 nm.

Table 1. J-V characteristic parameters of CdSe (sample c) QDSSCs for different dipping times.

Dipping time (h)	V_{oc} (Volt)	J_{sc} (mA/cm^2)	FF	Efficiency (η) ($\pm$0.01) %
1	0.51	0.44	0.48	0.11
3	0.53	0.47	0.40	0.13
6	0.50	1.62	0.48	0.29
24	0.54	0.62	0.60	0.20

The values of V_{oc}, J_{sc}, FF, and η of the assembled QDSSCs are given in Table 1. It is observed that both J_{sc} and η increase as the dipping time increases up to 6 hours, peaking at 1.62 mA/cm^2 and 0.29 % respectively. These values decreased to 0.62 mA/cm^2 and 0.20 % for 24 hour dipping time. All other CdSe QDs sizes showed the same behavior. These results could be explained in terms of the dipping time: as the time increases above 6 hours, there is an additional amount of CdSe QDs loaded, leading to blocking the nanopores of TiO_2 layer, and the reduction of both J_{sc} and η. Similarly, Prabakar *et al.* [33] made the measurements of J_{sc}, and η of CdS QDs onto TiO_2 NPs by CBD technique. In their work, they found that J_{sc} and η obtained in 1 minute deposition time were better than those produced in longer dipping times. In our work, the optimum dipping time of 6 h is due to the fact that DA process needs longer time to be optimized than CBD technique. The relatively long adsorption time in DA helps in reducing the limiting effect of many parameters such as surface solution cleanliness, and QD concentration in the dispersion of TiO_2.

Fig. 6 shows the J-V characteristics of the assembled CdSe QDSSCs, constructed from the different sized CdSe QDs (a to e) for the same dipping time of 6 hours, under 1.5 AM illumination. Table 2 gives characteristic parameters of the assembled cells.

It is clearly seen that as CdSe QDs size increases, reaching 4.54 nm for sample (c), the values of J_{sc} and η increase, peaking at 1.62 mA/cm^2 and 0.29 % respectively. These values decrease for sample (d) (0.62 mA/cm^2 and 0.17 %) and (e) (0.44 mA/cm^2 and 0.13 %). These results are caused by two opposite effects influencing the photocurrent generation for the assembled cells. The first effect, the decrease in the particle size, results in a blue shift and thus causes relatively lower absorption of the incident photons from the solar spectrum. Therefore, the CdSe QDs of 4.54 nm size that correspond to 542 nm onset of absorption spectra are compatible to the maximum of the solar intensity spectrum [34] and therefore can harvest more visible photons than QDs with the sizes of 4.32 and 4.02 nm. The second effect is the energetic alignments of CdSe QDs and those of TiO_2 NPs, which can be deduced from the EMA model (Eq. 1). In this Equation, the third term represents the Coulomb energy, which is generally a very small quantity compared with the

Table 2. J-V characteristic parameters of CdSe QDSSCs for different QDs sizes, at 6 hours dipping time, under 1 sun illumination.

CdSe QDs Size (nm)	QD Band Gap Energy (eV)	V_{oc} (Volt)	J_{sc} (mA/cm^2)	FF	Efficiency (η) ($\pm$0.01) %
4.02	2.44	0.51	0.51	0.42	0.11
4.32	2.33	0.49	1.04	0.51	0.26
4.54	2.26	0.50	1.62	0.48	0.29
4.84	2.19	0.50	0.62	0.56	0.17
5.20	2.13	0.52	0.44	0.55	0.13

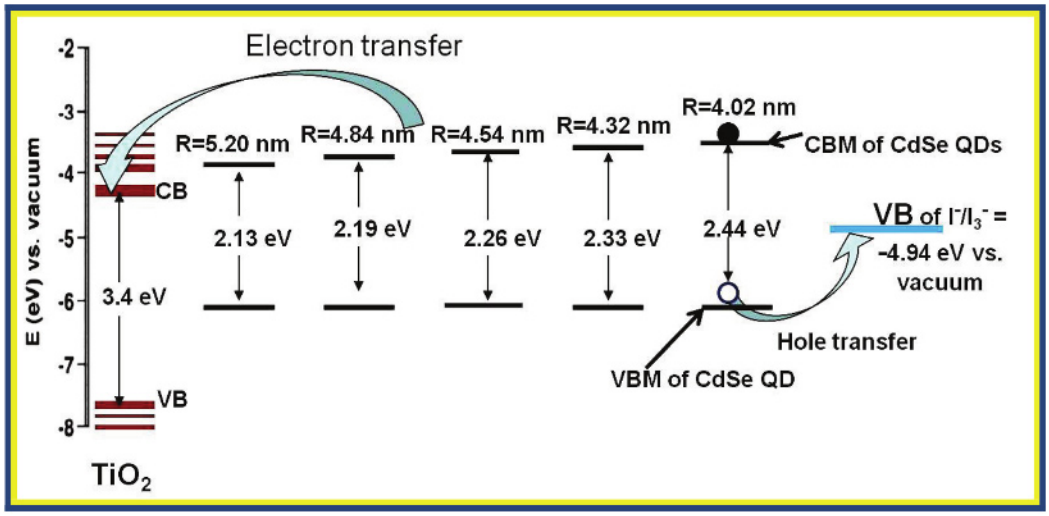

Fig. 7. Summary of energy diagram showing the alignment of the VBM and CBM of CdSe QDs with respect to TiO_2 valence and conduction bands (all data *vs.* vacuum).

kinetic energy (second term), hence, we can neglect it [35]. The energy variation of the conduction band minimum (CBM) (the lowest unoccupied molecular orbital (LUMO) levels) is inversely proportional to m_e, while the valance band maximum (VBM) (the highest occupied molecular orbital (HOMO) levels) is also inversely proportional to m_h as shown in the following equations [36, 37]:

$$\Delta E_{\mathrm{CBM}} = \frac{h^2}{8m_e R^2} \tag{2}$$

$$\Delta E_{\mathrm{VBM}} = -\frac{h^2}{8m_h R^2} \tag{3}$$

Since m_e is much smaller than m_h, thus the variation in the values of CBM are significantly larger than that of VBM. Using Eqs. 2 and 3, the values of ΔE_{CBM} were calculated as 0.72, 0.62, 0.56, 0.50, and 0.44 eV, and ΔE_{CBM} as -0.20, -0.18, -0.16, -0.14, and -0.13 eV for CdSe QDs (a to e) respectively. The value of the CB of bulk CdSe (-4.3 eV *vs.* vacuum) as deduced from electron affinity [25], is very close to the CB of TiO_2 (-4.3 eV *vs.* vacuum) [38]. The valance band (VB) for bulk CdSe, is -6.04 eV *vs.* vacuum [25], which is well below the VB of the redox potential of I^-/I_3 (-4.94 eV *vs.* vacuum) [20]. The energetic alignments diagram of CdSe QDs adsorbed onto the TiO_2 NPs surface is shown in Fig. 7. It is easily observed that as the size of QDs decreases, the CB shifts to more negative potential, which causes an increase in the driving force. Consequently, the electrons injection to TiO_2 NPs becomes faster, leading to an increase of the J_{sc}, and finally enhances η. The increase in the values of J_{sc} and η, seen as the size decrease from 5.20 to

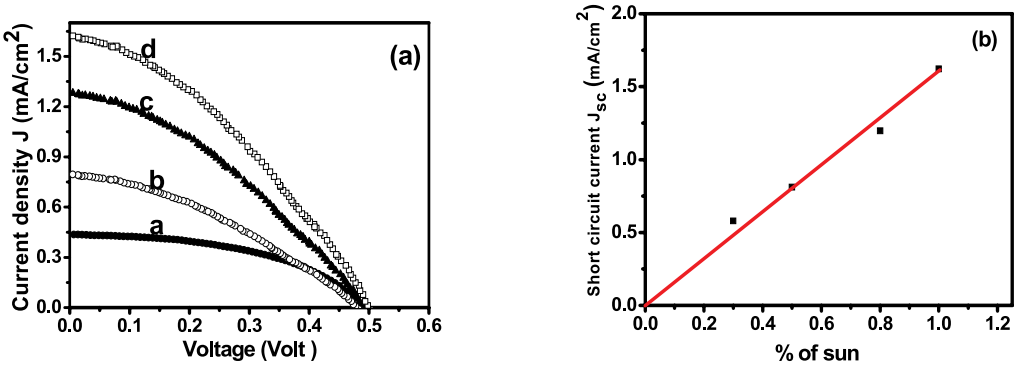

Fig. 8. (a) J-V characteristics curve of a CdSe (sample c) QDSSC for 6 hours dipping time at: a) 30 %, b) 50 %, c) 80 %, and d) 100 % of sun; (b) short circuit current density J_{sc} *vs.* the percentage of sun.

4.54 nm of CdSe particles, supports this reasoning. Our results show that these two competing effects are combined for the particle size of the radius of 4.54 nm.

The VBM variations of CdSe QDs are approximately the same for all sizes of the samples ($\Delta E_{\mathrm{CBM}} < -0.2$ eV). This variation lowers the VB of bulk CdSe (6.04 eV) [25, 39], and therefore, the regeneration of CdSe QDs by the redox couple in the electrolyte is energetically favored since the electrolyte VB (−4.95 eV *vs.* vacuum [20]) is larger than that of the VBM of CdSe QDs, as shown in Fig. 7. Furthermore, it is seen that V_{oc} (0.50 ± 0.02 volt) is independent of CdSe QDs size. This occurs since the electrons are injected quickly from the CBM of CdSe QDs to the lower CB energy of TiO_2 NPs, indicating that the CB level of TiO_2 NPs and the VB of the electrolyte decide about V_{oc} of the assembled QDSSCs. In addition, the DA technique, which is used to deposit CdSe QDs onto TiO_2 NPs, leads to matching the CdSe QDs bands to that of TiO_2 NPs without any barriers, which results in a direct electronic interaction between the two semiconductor materials (CdSe QDs and TiO_2 NPs). So, DA technique minimizes the electrons injection time from CBM of CdSe QDs to that of TiO_2 NPs.

Fig. 8(a) shows the performance of the assembled CdSe (sample c) QDSSCs at various intensities of solar illumination (from 0–100 %). The J-V characteristics curves were recorded for the 6 hour dipping time assembly. It is seen that as the intensity of the incident light increases, the measured J_{sc} increases linearly due to increased electrons injection, as shown in Fig. 8(b). The approximately constant value of V_{oc} indicates the high sensitivity of CdSe QDSSCs that was prepared by DA method.

4. Conclusions

Pre-synthesized CdSe QDs of different sizes were adsorbed onto TiO_2 NPs electrode using the direct adsorption (DA) method, for different dipping times up to 24 h, as a sensitizer for photovoltaic cell. The reduction of both J_{sc} and η as the dipping time increased above 6 h are due to blocking the nanopores of TiO_2 layer by the additional amount of the loaded CdSe QDs. The maximum values of short circuit current density (J_{sc}) and conversion efficiency (η) are 1.62 mA/cm^2 and 0.29 % respectively, corresponding to 542 nm absorption edge of CdSe QDs (size 4.54 nm) at 6 h dipping time, and AM 1.5 simulated sunlight. Our results show that this particle size connects the faster electron injection rate of small size particle and greater absorption range of large size particle effectively. Furthermore, as the intensity of the incident solar light increases, J_{sc} increases linearly, indicating greater sensitivity of the CdSe QDSSCs.

Acknowledgements

The authors wish to thank Quantum Optics Research Group (QORG) at Taif University for their assistance during this work. One of the authors (H. Talaat) appreciates the support of the Egyptian STDF (grant ID377).

References

[1] KAMAT P.V., *J. Phys. Chem. C*, 112 (2008), 18737.

[2] BASKOUTAS S., TERZIS A.F., *Mat. Sci. Eng. B*, 147 (2008), 280.

[3] XIE Y., YOO S. H., CHEN C., CHO S.O., *Mat. Sci. Eng. B*, 177 (2012), 106.

[4] TVRDY K., FRANTSUZOV P.A., KAMAT P.V., *PNAS*, 108 (2011), 29.

[5] IKHMAYIES S.J., AHMAD-BITAR R.N., *Sol. Energy Mater. Sol. Cells*, 94 (2010), 878.

[6] LI Y., PANG A., ZHENG X., WEI M., *Electrochim. Acta*, 56 (2011), 4902.

[7] KIM J. *et al.*, *J. Power Sources*, 196 (2011), 10526.

[8] SHEN Q., YANAI M., KATAYAMA K., SAWADA T., TOYODA T., *Chem. Phys. Lett.*, 442 (2007), 89.

[9] TUBTIMTAE A., WU K.-L., TUNG H.-Y., LEE M.-W., WANG G.J., *Elec. Comm.*, 12 (2010), 1158.

[10] YUM J.-H., CHOI S.-H., KIM S.-S., KIM D.-Y., SUNG Y.-E., *J. Korean Phys. Soc.*, 10 (2007), 257.

[11] PERNIK D.R., TVRDY K., RADICH J.G., KAMAT P.V., *J. Phys. Chem. C*, 115 (2011), 13511.

[12] NOZIK A.J., *Chem. Phys. Lett.*, 457 (2008), 3.

[13] GEBRESELASSIE H.M., SHARMA R.B., *Int. J. Eng. Sci. and Technology (IJEST)*, 3 (2011), 2073.

[14] GUIJARRO N., LANA-VILLARREAL T., MORA-SERÓ I., BISQUERT J., GÓMEZ R., *J. Phys. Chem. C*, 113 (2009), 4208.

[15] CHEN H., LI W., LIU H., ZHU L., *Elec. Comm.*, 13 (2011), 331.

[16] LANDI B.J., CASTRO S.L., RUF H.J., EVANS C.M., BAILEY S.G., RAFFAELLE R.P., *Sol. Energy Mater. Sol. Cells*, 87 (2005), 733.

[17] BADAWI A., AL-HOSINY N., ABDALLAH S., NEGM S., TALAAT H., *J. Mat. Sci. Eng. A*, 1 (2011), 942.

[18] KITADA S., KIKUCHI E., OHNOB A., ARAMAKIB S., MAENOSONO S., *Solid State Communications*, 149 (2009), 1853.

[19] LIU Y., WANG J., *Thin Solid Films*, 518 (2010), e54.

[20] YU P., ZHU K., NORMAN A.G., FERRERE S., FRANK A.J., NOZIK A.J., *J. Phys. Chem. B*, 110 (2006), 25451.

[21] WANG C.-C., CHEN L.-C., WANG T.-C., *J. Optoelectronics Advanced Mat.*, 11 (2009), 834.

[22] LIN M.-C., LEE M.-W., *Elec. Comm.*, 13 (2011), 1376.

[23] TUBTIMTAE A., LEE M.-W., WANG G.-J., *J. Power Sources*, 196 (2011), 6603.

[24] MADELUNG O., *Semiconductors: Data Handbook*, Springer-Verlag, Berlin, 2004.

[25] JASIENIAK J. *et al.*, *Advanced Functional Materials*, 17 (2007), 1654.

[26] MORA-SERÓ. I. *et al.*, *Nanotechnology*, 19 (2008), 424007.

[27] RUHLE S., SHALOM M., ZABAN A., *Chem. Phys. Chem.*, 11 (2010), 2290.

[28] SALANT A., SHALOM M., HOD I., FAUST A., ZABAN A., BANIN U., *ACS NANO*, 4 (2010), 5962.

[29] KONGKANAND A., TVRDY K., TAKECHI K., KUNO M., KAMAT P.V., *J. Am. Chem. Soc.*, 130 (2008), 4007.

[30] TALAPIN D.V., HAUBOLD S., ROGACH A.L., KORNOWSKI A., HAASE M., WELLER H., *J. Phys. Chem. B*, 105 (2001), 2260.

[31] SYRROKOSTAS G., GIANNOULI M., YIANOULIS P., *Renewable Energy*, 34 (2009), 1759.

[32] THAMBIDURAI M., MURUGAN N., MUTHUKUMARASAMY N., VASANTHA S., BALASUNDARAPRABHU R., AGILAN S., *Chalcogenide Letters*, 6 (2009), 171.

[33] PRABAKAR K., SEO H., SON M., KIM H., *Mater. Chem. Phys.*, 117 (2009), 26.

[34] DAVID I., in: M.L. Trevor (Ed.), *Future Energy*, Elsevier, Oxford, 2008, p. 225.

[35] NANDAKUMAR P., VIJAYAN C., MURTI Y.V.G.S., *J. Appl. Phys.*, 91 (2002), 1509.

[36] MALL M., KUMAR P., CHAND S., KUMAR L., *Chem. Phys. Lett.*, 495 (2010), 236.

[37] BLACKBURN J.L., SELMARTEN D.C., ELLINGSON R.J., JONES M., MICIC O., NOZIK A.J., *J. Phys. Chem. B*, 109 (2005), 2625.

[38] KNIPRATH R., RABE J.P., MCLESKEY J.T. JR., WANG D., KIRSTEIN S., *Thin Solid Films*, 518 (2009), 295.

[39] HYUN B.-R. *et al.*, *ACS NANO*, 2 (2008), 2206.

Received: 2012-04-29
Accepted: 2012-11-03